Mixed Coordination Silica at Megabar Pressure

Cong Liu,[1] Jiuyang Shi,[1] Hao Gao,[1] Junjie Wang,[1] Yu Han,[1] Xiancai Lu,[2] Hui-Tian Wang,[1] Dingyu Xing,[1] and Jian Sun[1,*]

[1]National Laboratory of Solid State Microstructures, School of Physics, and Collaborative Innovation Center of Advanced Microstructures, Nanjing University, Nanjing 210093, China

[2]State Key Laboratory for Mineral Deposits Research, School of Earth Sciences and Engineering, Nanjing University, Nanjing 210093, China

(Received 22 September 2020; accepted 24 December 2020; published 20 January 2021)

Silica (SiO_2), as a raw material of silicon, glass, ceramics, abrasive, and refractory substances, etc., is of significant importance in industrial applications and fundamental research such as electronics and planetary science. Here, using a crystal structure searching method and first-principles calculations, we predicted that a ground state crystalline phase of silica with $R\bar{3}$ symmetry is stable at around 645–890 GPa, which contains six-, eight-, and nine-coordinated silicon atoms and results in an average coordination number of eight. This mixed-coordination silica fills in the density, electronic band gap, and coordination number gaps between the previously known sixfold pyrite-type and ninefold Fe_2P-type phases, and may appear in the core or mantle of super-Earth exoplanets, or even the solar giant planets such as the Neptune. In addition, we also found that some silicon superoxides, *Cmcm* SiO_3 and *Ccce* SiO_6, are stable in this pressure range and may appear in an oxygen-rich environment. Our finding enriches the high-pressure phase diagram of silicon oxides and improves understanding of the interior structure of giant planets in our solar system.

DOI: 10.1103/PhysRevLett.126.035701

Silica (SiO_2), as the most abundant mineral in the Earth's crust, is of great importance for our understanding of planetary formation and composition [1–3]. Exploration for new phases of silica has attracted substantial interests in many fields, such as geophysics, condensed matter physics, and material science [4–13], etc. In silica crystals, each silicon atom is coordinated by oxygen atoms and form different kinds of polyhedra (e.g., SiO_4, SiO_6, and SiO_9), corresponding to silicon atom coordination numbers (CN) of 4, 6, and 9, respectively. High pressure studies have shown that silica has a rich phase diagram with increasing coordination number for silicon atoms under compression. For instance, low-pressure polymorphs of silica, such as quartz and coesite, are basically composed by SiO_4 tetrahedra. At ~10 GPa, the coordination number of silicon atoms increases to 6, and then a sequence of pressure-induced phase transitions in silica emerge in turn: rutile-type → $CaCl_2$-type → α-PbO_2-type → pyrite-type. Up to now, the pyrite-type structure has been observed in experiments up to 271 GPa [12]. In addition, theoretical studies [14,15] suggested that the pyrite-type structure will transform into a Fe_2P-type structure at ~690 GPa, in which silicon atoms are all located inside SiO_9 polyhedra (CN = 9). Quasiharmonic approximation (QHA) calculations showed that another ninefold crystal, the cotunnite-type structure, is competitively more stable than the Fe_2P-type structure at higher temperature in a similar pressure range. With compression up to 10 TPa, silica in the Fe_2P-type structure will transform into a tenfold *I4/mmm* structure, similar to the pressure induced phase transition sequence of TiO_2 [16].

In the group IV–VI compounds, theoretical calculations [17] suggested that in several isovalent AB_2 compounds (CO_2, CS_2, SiO_2, SiS_2, and GeO_2), the group-IV atoms all refuse to form structures with sevenfold and eightfold coordination, and the only eight-coordinated silicon atoms appear in the SiS structure, which is decomposed from SiS_2 under compression. Although experiments have not found any evidence for high coordination numbers larger than 6 of silicon atoms in the ground states of silica crystalline phases, signatures for a continuous increase of the silicon atom coordination number greater than six have been observed in the silica glassy state [18,19]. Moreover, experiments also found fivefold or sixfold mixed coordination in a metastable silica phase [20] in the pressure range between the fourfold and sixfold silica crystalline phases.

As aforementioned, there is an obvious gap in the coordination number between the sixfold pyrite-type and the ninefold Fe_2P-type structure. How the coordination number of silica evolves in the pressure range under the planetary core condition, and whether there is any mixed-coordination ground state are still open questions. To address these questions, we explore the new crystalline structures of silica and its possible decompositions in the pressure range of planetary core conditions by a crystal

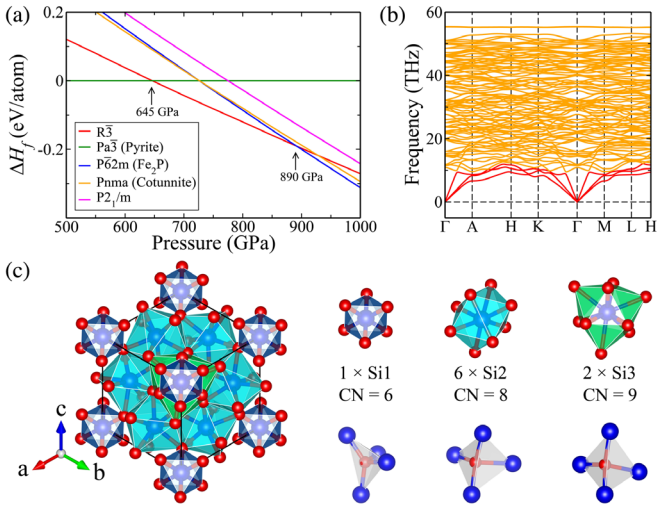

FIG. 1. Energetics, dynamical stability, and crystal structures of the $R\bar{3}$ phase silica. (a) Enthalpies of the silica phases of interest relative to the pyrite-type structure in the pressure range between 500 and 1000 GPa. (b) Phonon spectra of the $R\bar{3}$ phase at 700 GPa. Red and orange lines represent the acoustic and optical branches, respectively. (c) Crystal structure of the predicted $R\bar{3}$ phase, where blue and red spheres represent Si and O atoms, respectively. There are three kinds of different polyhedra containing silicon atoms of sixfold (Si1, blue), eightfold (Si2, cyan), and ninefold (Si3, green), respectively, and all oxygen atoms are fourfold and form tetrahedra (white).

structure prediction method and first-principles calculations. Very interestingly, we find a rhombohedral ground-state silica phase with mixed coordination of six, eight and nine, as well as some silicon superoxides, such as SiO_3 and SiO_6. These newly found compounds are stable in a large pressure range and may appear in the core of planets, such as Neptune and super-Earths.

We used an in-house code called Magus (machine learning and graph theory assisted universal structure searcher), in which we employed the Bayesian optimization [21] and graph theory to improve the search efficiency and diversity. This method has been successfully applied in many systems, including compounds inside planets [22–24]. DFT calculations were performed with the Vienna *ab initio* simulation package (VASP) [25], accompanied with the projector augmented-wave (PAW) method [26]. We chose $3s^2 3p^2$ and $2s^2 2p^4$ as valence electrons for Si and O, and used the generalized gradient approximation (GGA) in the Perdew-Burke-Ernzerhof (PBE) exchange correlation functional [27].

We have searched extensively for new silica crystal structures in the pressure range of 500–1000 GPa and found several energetically competitive candidates. Enthalpy calculations show that rather than the previously known pyrite-type and Fe_2P-type silica, a new rhombohedral crystalline structure of silica with $R\bar{3}$ symmetry is energetically the most stable from 645 to 890 GPa, as shown in Fig. 1(a). Phonon calculations [28] show that there are no imaginary modes above 100 GPa, e.g., see Figs. 1(b) and S1 in the Supplemental Material [29], confirming the robust dynamic stability of this $R\bar{3}$ phase under high pressure.

Surprisingly, unlike other silica crystalline phases with unique coordination number of silicon atoms, this $R\bar{3}$ phase adopts mixed coordination numbers. As shown in Fig. 1(c), there are three kinds of Si atoms, accompanied with three different kinds of polyhedra. One Si atom (marked as Si1) at 1a (0, 0, 0) is six coordinated and forms one SiO_6 octahedron with point group D_{3d}. While six Si atoms (Si2) are eight coordinated and form SiO_8 dodecahedra, and two Si atoms (Si3), located on the body diagonal line in the (1 1 1) direction, are nine coordinated and form SiO_9 polyhedra. At 700 GPa, the SiO_6 octahedra share only one type of Si-O bond length, which is about 1.50 Å. While the SiO_8 dodecahedra and SiO_9 polyhedra are both highly distorted, their Si-O bond lengths are ranging from 1.52 to 1.78 Å and from 1.53 to 1.84 Å, respectively. As shown in Table I in Supplemental Material [29], this $R\bar{3}$ silica has a moderate polyhedral occupancy ($\sum V_{\mathrm{poly}}/V_{\mathrm{cell}}$) of 0.62, which is between that of the pyrite-type (0.36) and the Fe_2P-type/cotunnite-type silica (0.79/0.78). Different from the pyrite-type silica in which each O atom is all coordinated by three Si atoms, the O atom in the $R\bar{3}$ phase is all folded by four Si atoms, on the other hand, indicating that the average coordination number for the silicon atoms should be eight. The crystal structure information and bulk modulus of the $R\bar{3}$ phase can be found in the Supplemental Material [29]. Given that there exists three types of Si atoms with the ration of 6:2:1 in the $R\bar{3}$ silica, we searched for analogous compounds from the Materials Project database [30] using a formula of $AB_2C_6D_{18}$ and $R\bar{3}$ symmetry, and found five crystals exhibiting a similar pattern: $K_2Ge(IO_3)_6$, $Cs_2Zr(IO_3)_6$, $Rb_2Zr(IO_3)_6$, $Rb_2Mo(IO_3)_6$, and $TiAg_2(IO_3)_6$, among which the first three are ground state structures at ambient condition according to the database.

We also found several other candidates for the high-pressure phases of silica with coordination numbers between six and nine, their enthalpy-pressure relations and crystal structures can be found in Figs. S2 and S3 in the Supplemental Material [29]. Especially, the $P\bar{3}$ and *Cmce* phase silica are also mixed coordination structures. And then, when we try to quench the mixed coordination $R\bar{3}$ silica to the ambient pressure, it will transform into a metastable $P\bar{3}1m$ structure at around 60 GPa with structural optimizations; more details about this structure can be found in Figs. S4 and S5 in the Supplemental Material [29].

As shown above, from the pyrite-type to the Fe_2P-type silica, there is an obvious gap of polyhedral occupancy; this inspired us to look into the equation of state of the silica phases. As shown in Fig. 2(a), in the pressure range of interest, the densities of all the four relevant phases are sensitive to the pressure and have similar slopes

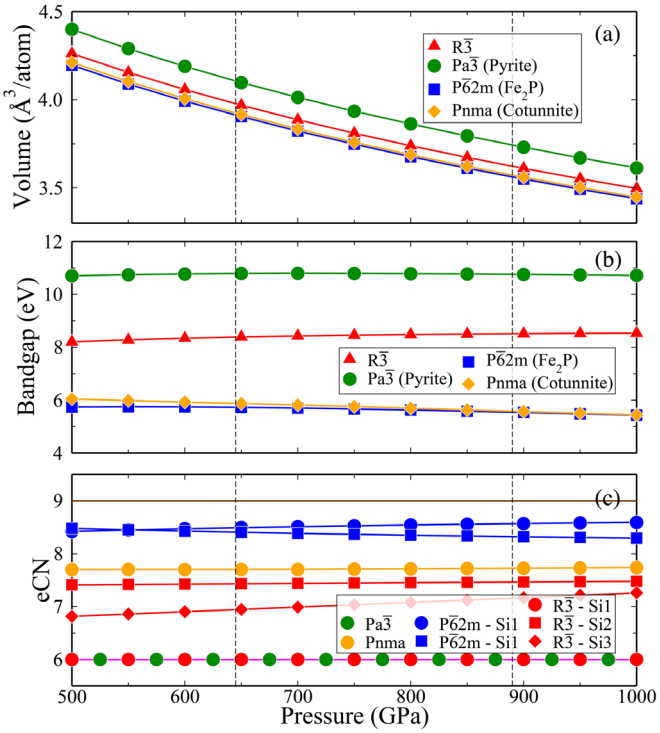

FIG. 2. Compression behaviors of the interested silica phases under high pressures, including (a) density, (b) band gap, and (c) effective coordination number analysis. Vertical dashed lines denote the silica phase transition pressures from the pyrite-type to the $R\bar{3}$ phase and from the $R\bar{3}$ phase to the Fe_2P-type. Magenta (brown) line in (c) corresponds to the ideal sixfold (ninefold) of silicon atoms in the silica crystals.

of compressibility. However, the packing efficiency and density of the $R\bar{3}$ phase silica are between that of the sixfold (pyrite-type) and the ninefold (Fe_2P-type and cotunnite-type) structures. It is not surprising since the $R\bar{3}$ phase is a mixed coordination phase with sixfold, eightfold, and ninefold. This indicates that the $R\bar{3}$ phase is an intermediate structure between the sixfold and ninefold silica. On the other hand, as can be seen in Fig. 2(b), the electronic band gap of the $R\bar{3}$ phase is also between that of the sixfold and the ninefold structures. In additional, it has a positive pressure dependence, increasing with pressure from around 8.20 eV at 500 GPa to 8.53 eV at 1000 GPa. Meanwhile, the Fe_2P-type and cotunnite-type structures (both ninefold) are very closely related with each other, both on energy and crystal structure [15], leading to the fact that their densities and band gaps are highly degenerate.

As discussed above, after adding our newly found $R\bar{3}$ phase, the density, band gap, and coordination number of Si atoms in silica increases more gradually under compression. As shown by Tsuchiya *et al.* [14], the distortion of the SiO_x polyhedra can be reflected by a quantity called effective coordination number (eCN). For instance, in the pyrite-type structure all SiO_6 polyhedra share only one Si-O bond length (see Table II in the Supplemental Material [29]) and thus the silicon atoms are the ideal sixfold and the polyhedra have no distortion, resulting in an eCN of 6.0, as shown in Fig. 2(c). While the SiO_9 polyhedra in the Fe_2P and cotunnite structures are quite distorted, and their eCNs are much lower than ideal 9, consistent with those in Ref. [14]. As an intermediate structure between the pyrite-type and Fe_2P-type phases, the situation in the $R\bar{3}$ phase is even more complicated, exhibiting some combinational features. For instance, the SiO_6 polyhedra in the $R\bar{3}$ phase have only one Si-O bond length and an ideal eCN of 6.0, which is independent of pressure. While the SiO_8 and SiO_9 polyhedra in the $R\bar{3}$ silica are highly distorted, and their eCNs are even lower than that of the SiO_9 polyhedra in the Fe_2P-type and cotunnite-type structures. Meanwhile, the Si–O bond lengths in the $R\bar{3}$ silica (varied from 1.52 to 1.81 Å at 700 GPa) are even comparable to that of quartz at ambient pressure (∼1.6), which indicates that the pressure-induced phase transition to the $R\bar{3}$ phase in silica is achieved not only by shrinking the Si1–O bond length of SiO_6 polyhedra, but also by the increase of the coordination numbers (Si2 in SiO_8 polyhedra and Si3 atoms in SiO_9 polyhedra) and the polyhedral occupancy. As shown in Table III of the Supplemental Material [29], both the $R\bar{3}$ and the Fe_2P phases show nonsingle charge occupations instead of the only one type of charge of the silicon atoms in the pyrite and cotunnite phases.

Inspired by the mixed coordination numbers in the silica crystal structure, we have extended our crystal structure searches to explore different stoichiometry in the Si-O system. If any new compound exists, it should have lower formation enthalpy than the mixture of the most stable phases of silica (pyrite-, Fe_2P-, and cotunnite-tye) [11,12,14,15] and solid oxygen [31] at the corresponding pressures. Interestingly, our calculated convex hulls show that two superoxide compositions, SiO_3 and SiO_6, are beginning to gain their thermodynamic stability at around 500 GPa and survive up to at least 1 TPa, as shown in Fig. 3(a). Static formation enthalpy calculations (as shown in Fig. S6 in Supplemental Material [29]) indicate that the SiO_3 compound becomes thermodynamically stable above 524 GPa. It forms a previously reported $I\bar{4}$ phase [32] and then can transform into a new *Cmcm* phase at around 800 GPa. In addition, the SiO_6 compound becomes thermodynamically stable above 490 GPa and maintains a *Ccce* structure in the whole pressure range we investigated, as shown in Figs. 3(b) and S7 in Supplemental Material [29]. Interestingly, all the crystal structures of the SiO_3 and SiO_6 do not have mixed coordination. For instance, in the *Cmcm* SiO_3 crystal, all silicon atoms form SiO_9 polyhedra with a small eCN of 7.84 at 700 GPa, very close to that in the cotunnite-type silica. In the *Ccce* phase of SiO_6, all the silicon atoms form SiO_8 polyhedra with an eCN of 7.96 at 700 GPa, very close to the ideal eCN of 8. As shown in the Figs. S8 and S9 in Supplemental Material

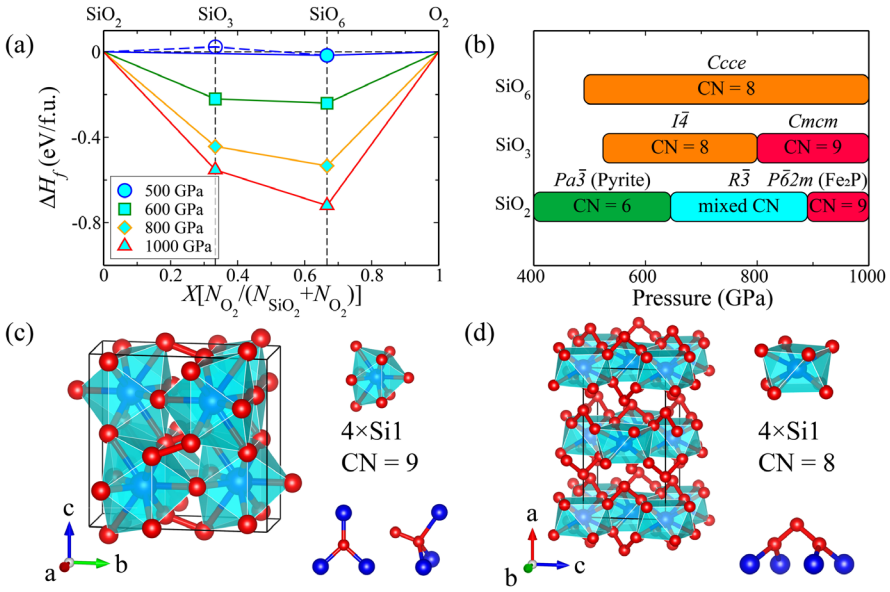

FIG. 3. Energetics of the Si-O system and crystal structures of the most stable compounds at 400–1000 GPa. (a) Convex hulls for formation enthalpies (ΔH_f, relative to the most stable phases of SiO_2 [11,12,14,15] and O_2 [31]) at different pressures. (b) Pressure-composition phase diagram of the Si-O compounds from 400 to 1000 GPa. The crystal structures of the *Cmcm* phase SiO_3 (c) and the *Ccce* phase SiO_6 (d) at 700 GPa, as well as corresponding coordination of silicon and oxygen atoms.

[29], phonon calculations show that both SiO_3 and SiO_6 are dynamically stable, and therefore such exotic silicon superoxides can gain stability in an oxygen-rich environment.

As such mixed coordination silica, as well as other two exotic silicon superoxides, are stable under the high-pressure condition in the core or core-mantle boundary of super-Earth-type exoplanets. Thus, we modeled the evolutions of these compounds at finite pressure and temperature conditions in the core or interior mantle of the possible super earth. We can figure out the most stable structures under finite temperature from Gibbs free energy curves, as shown in Fig. S10 in the Supplemental Material [29]. A summary of our calculations up to 10000 K gives an ultrahigh pressure-temperature phase diagram of silica crystal, see Fig. 4(a). Compared to the previously proposed phase diagram [14], in our newly proposed phase diagram, the stable region of the pyrite-type structure and even the slop of the boundary line between the pyrite-type and post-pyrite-type structure do not change too much. However, the appearance of the $R\bar{3}$ phase significantly decreases the stable range of the cotunnite structure and also increases the pressure at which the Fe_2P phase appears from ~720 to ~890 GPa. At low temperatures, the $R\bar{3}$ phase of silica directly transforms into the Fe_2P structure. Whereas at the temperature higher than 3600 K, the cotunnite structure begins to appear in the region between the $R\bar{3}$ structure and Fe_2P phase. Similar to the previously proposed phase diagram [14], the cotunnite-Fe_2P phase boundary has a positive slope. However, the slope of the $R\bar{3}$-cotunnite phase boundary and the $R\bar{3}$-Fe_2P phase boundary lines are both negative.

In addition, the adiabatic geotherms (brown and blue squares) suggested for the super-Earths [34] are also plotted in Fig. 4(a) to represent pressure-temperature conditions at core-mantle boundary (CMB) with different interior composition. Along the geotherm, the pyrite-type, $R\bar{3}$ phase, cotunnite-type, and Fe_2P-type silica emerge sequentially, and the $R\bar{3}$ phase silica can therefore be expected to appear inside a massive super-Earth between ~5 $M_\oplus$ and ~7 $M_\oplus$ in the terrestrial form or between ~5.5 $M_\oplus$ and ~7.5 $M_\oplus$ in the ocean form super-Earth. As reported in previous work [35,36], if one considers the dissociations of $MgSiO_3$, the adiabatic geotherm of terrestrial type exoplanets [green circles in Fig. 4(a)] are highly changed. Take this into account, then the $R\bar{3}$ silica predicted in this work should survive between ~4.2 $M_\oplus$ and ~5.5 $M_\oplus$. The CMBs of the solar planets obtained from different groups [37,38] are slightly different, and according to the model proposed by Nettelmann *et al.* [38], the CMBs of Neptune are located nicely in the $R\bar{3}$ phase region, which shows the possibility that this $R\bar{3}$ silica is widespread in the universe. According to the melting line of silica from the shock wave compression experiment [33], the silica phases at the CMB conditions of these planets should still be solids. In addition, previous works [2] showed that the post-perovskite $MgSiO_3$ may disassociate into MgO and SiO_2 at ~1000 GPa. Considering that the competition between the $R\bar{3}$ silica and Fe_2P-type (cotunnite-type) phase is in the pressure range from 645 to 890 GPa, thus the mixed coordination structure of silica will not affect the disassociation reactions of $MgSiO_3$.

As for the *Cmcm* phase of SiO_3 and the *Ccce* phase of SiO_6 at high pressures, they are very temperature sensitive

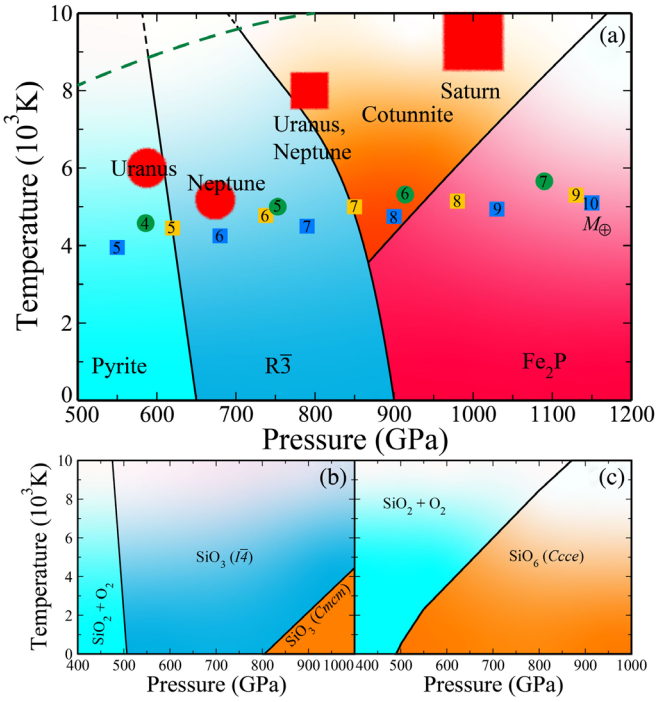

FIG. 4. Proposed pressure-temperature phase diagrams of (a) silica, (b) SiO_3, and (c) SiO_6 at planetary core conditions. The melting curve (dark green dashed line) of silica is obtained from shock wave experiments [33]. The phase boundary lines are marked with black solid lines and dashed boundaries (indicate pressure-temperature conditions out of the QHA validity range). Small brown or blue squares represent the pressure-temperature conditions at the core-mantle boundary (CMB) in terrestrial or ocean type exoplanets by Sotin *et al.* [34], and green circles represent the CMB conditions in terrestrial type exoplanets by Hakim *et al.* [35] and van den Berg *et al.* [36], respectively. Numbers inside the small squares and circles represent the planet mass in units of Earth mass ($M_\oplus$). Red squares and circles denote the estimated pressure-temperature conditions at CMB in the solar giant planets (e.g., Uranus, Neptune, and Saturn), respectively, by Guillot *et al.* [37] and Nettelmann *et al.* [38].

and both of them have a boundary with sharp negative slope, as shown in Figs. 4(b) and 4(c). Especially, the SiO_6 is a completely new stoichiometry that has never been reported before, and may exist under ultrahigh pressure and temperature, especially in an oxygen-rich environment. They may have significant effects on the formation and disassociation of minerals, such as $MgSiO_3$, Mg_2SiO_4, and $MgSi_2O_5$ in super-Earth mantles [1,2,39]. Investigations on this would need elaborate crystal structure searches in the whole Mg-Si-O ternary system, which is beyond the scope of this work and will be reserved for future studies.

In summary, using a machine learning accelerated crystal structure prediction and *ab initio* calculations, we found a new ground state crystalline phase of silica with $R\bar{3}$ symmetry in the pressure range from 645 to 890 GPa. This $R\bar{3}$ phase perfectly fills the gaps of density and polyhedral occupancy between the sixfold pyrite-type and ninefold Fe_2P-type silica, in which three kinds of silicon atoms are coordinated with different numbers of oxygen atoms and form the SiO_6, SiO_8, and SiO_9 polyhedra, respectively, finally resulting in an average coordination number of eight. The electronic band gap of the $R\bar{3}$ phase is between those of the pyrite-type and Fe_2P-type silica, and exhibits an abnormal increase with compression. In addition, we also found a ninefold *Cmcm* SiO_3 phase and an eightfold *Ccce* phase SiO_6. And we proposed the ultrahigh pressure-temperature phase diagrams of SiO_2, SiO_3, and SiO_6. The new phases predicted in this work are coincidently stable at the core conditions of giant planets such as Neptune, as well as super-Earth exoplanets, and thus these compounds may play a very important role in the research on the core or mantle of the super-Earths. Recent laser-driven shock experiments [33] have compressed the solid silica *to* pressures up to 700 GPa, which makes the experimental verification of the compounds predicted in this work possible.

J. S. gratefully acknowledges financial support from the National Key R&D Program of China (Grant No. 2016YFA0300404), the National Natural Science Foundation of China (Grant No. 11974162 and No. 11834006), and the Fundamental Research Funds for the Central Universities. The calculations were carried out using supercomputers at the High Performance Computing Center of Collaborative Innovation Center of Advanced Microstructures, the high-performance supercomputing center of Nanjing University, and "Tianhe-2" at NSCC-Guangzhou.

*Corresponding author.
jiansun@nju.edu.cn

[1] A. R. Oganov and S. Ono, Theoretical and experimental evidence for a post-perovskite phase of $MgSiO_3$ in Earth's D" layer, Nature (London) **430**, 445 (2004).
[2] K. Umemoto, R. M. Wentzcovitch, and P. B. Allen, Dissociation of $MgSiO_3$ in the cores of gas giants and terrestrial exoplanets, Science **311**, 983 (2006).
[3] K. Hirose, G. Morard, R. Sinmyo, K. Umemoto, J. Hernlund, G. Helffrich, and S. Labrosse, Crystallization of silicon dioxide and compositional evolution of the Earth's core, Nature (London) **543**, 99 (2017).
[4] Y. Tsuchida and T. Yagi, A new, post-stishovite high pressure polymorph of silica, Nature (London) **340**, 217 (1989).
[5] Y. Tsuchida and T. Yagi, New pressure-induced transformations of silica at room temperature, Nature (London) **347**, 267 (1990).
[6] K. J. Kingma, R. J. Hemley, H. K. Mao, and D. R. Veblen, New High-Pressure Transformation in α-Quartz, Phys. Rev. Lett. **70**, 3927 (1993).

[7] K. J. Kingma, R. E. Cohen, R. J. Hemley, and H. Mao, Transformation of stishovite to a denser phase at lower-mantle pressures, Nature (London) **374**, 243 (1995).

[8] L. S. Dubrovinsky, S. K. Saxena, P. Lazor, R. Ahuja, O. Eriksson, J. M. Wills, and B. Johansson, Experimental and theoretical identification of a new high-pressure phase of silica, Nature (London) **388**, 362 (1997).

[9] D. M. Teter, R. J. Hemley, G. Kresse, and J. Hafner, High Pressure Polymorphism in Silica, Phys. Rev. Lett. **80**, 2145 (1998).

[10] J. Haines, J. M. Léger, F. Gorelli, and M. Hanfland, Crystalline Post-Quartz Phase in Silica at High Pressure, Phys. Rev. Lett. **87**, 155503 (2001).

[11] A. R. Oganov, M. J. Gillan, and G. D. Price, Structural stability of silica at high pressures and temperatures, Phys. Rev. B **71**, 064104 (2005).

[12] Y. Kuwayama, K. Hirose, N. Sata, and Y. Ohishi, The pyrite-type high-pressure form of silica, Science **309**, 923 (2005).

[13] R. Martoňák, D. Donadio, A. R. Oganov, and M. Parrinello, Crystal structure transformations in SiO_2 from classical and ab initio metadynamics, Nat. Mater. **5**, 623 (2006).

[14] T. Tsuchiya and J. Tsuchiya, Prediction of a hexagonal SiO_2 phase affecting stabilities of $MgSiO_3$ and $CaSiO_3$ at multi-megabar pressures, Proc. Natl. Acad. Sci. U.S.A. **108**, 1252 (2011).

[15] S. Wu, K. Umemoto, M. Ji, C.-Z. Wang, K.-M. Ho, and R. M. Wentzcovitch, Identification of post-pyrite phase transitions in SiO_2 by a genetic algorithm, Phys. Rev. B **83**, 184102 (2011).

[16] M. J. Lyle, C. J. Pickard, and R. J. Needs, Prediction of 10-fold coordinated TiO_2 and SiO_2 structures at multi-megabar pressures, Proc. Natl. Acad. Sci. U.S.A. **112**, 6898 (2015).

[17] Y. Chen, X. Feng, J. Chen, X. Cai, B. Sun, H. Wang, H. Du, S. A. T. Redfern, Y. Xie, and H. Liu, Ultrahigh-pressure induced decomposition of silicon disulfide into silicon-sulfur compounds with high coordination numbers, Phys. Rev. B **99**, 184106 (2019).

[18] C. Prescher, V. B. Prakapenka, J. Stefanski, S. Jahn, L. B. Skinner, and Y. Wang, Beyond sixfold coordinated Si in SiO_2 glass at ultrahigh pressures, Proc. Natl. Acad. Sci. U.S.A. **114**, 10041 (2017).

[19] Y. Kono, Y. Shu, C. Kenney-Benson, Y. Wang, and G. Shen, Structural Evolution of SiO_2 Glass with Si Coordination Number Greater than 6, Phys. Rev. Lett. **125**, 205701 (2020).

[20] E. Bykova, M. Bykov, A. Černok, J. Tidholm, S. I. Simak, O. Hellman, M. P. Belov, I. A. Abrikosov, H.-P. Liermann, M. Hanfland, V. B. Prakapenka, C. Prescher, N. Dubrovinskaia, and L. Dubrovinsky, Metastable silica high pressure polymorphs as structural proxies of deep Earth silicate melts, Nat. Commun. **9**, 4789 (2018).

[21] K. Xia, H. Gao, C. Liu, J. Sun, H.-T. Wang, and D. Xing, A novel superhard tungsten nitride predicted by machine-learning accelerated crystal structure search, Sci. Bull. **63**, 817 (2018).

[22] C. Liu, H. Gao, Y. Wang, R. J. Needs, C. J. Pickard, J. Sun, H.-T. Wang, and D. Xing, Multiple superionic states in helium–water compounds, Nat. Phys. **15**, 1065 (2019).

[23] C. Liu, H. Gao, A. Hermann, Y. Wang, M. Miao, C. J. Pickard, R. J. Needs, H.-T. Wang, D. Xing, and J. Sun, Plastic and Superionic Helium Ammonia Compounds under High Pressure and High Temperature, Phys. Rev. X **10**, 021007 (2020).

[24] H. Gao, C. Liu, A. Hermann, R. J. Needs, C. J. Pickard, H.-T. Wang, D. Xing, and J. Sun, Coexistence of plastic and partially diffusive phases in a helium-methane compound, Natl. Sci. Rev. **7**, 1540 (2020).

[25] G. Kresse and J. Furthmüller, Efficient iterative schemes for ab initio total-energy calculations using a plane-wave basis set, Phys. Rev. B **54**, 11169 (1996).

[26] P. E. Blöchl, Projector augmented-wave method, Phys. Rev. B **50**, 17953 (1994).

[27] J. P. Perdew, K. Burke, and M. Ernzerhof, Generalized Gradient Approximation Made Simple, Phys. Rev. Lett. **77**, 3865 (1996).

[28] A. Togo and I. Tanaka, First principles phonon calculations in materials science, Scr. Mater. **108**, 1 (2015).

[29] See Supplemental Material at http://link.aps.org/supplemental/10.1103/PhysRevLett.126.035701 for more details about methods, crystal structures, phonon spectra, energetics, and charge transfers, etc. The mixed coordination silica phase belongs to space group $R\bar{3}$, $Z = 9$, lattice parameters: $a = 4.736$ Å, and alpha $= 95°$ at 700 GPa, Si atoms occupying the Wyckoff positions at 1a (0, 0, 0), 2c (0.6992, 0.6992, 0.6992), 6f (0.4543, 0.7674, 0.1123), and O atoms at 6f (0.8286, 0.4154, 0.9043), 6f (0.7780, 0.0420, 0.7660), 6f (0.5259, 0.8025, 0.4457). The bulk modulus of the $R\bar{3}$ phase is ~2.65 TPa from fitting the 3rd order Birch-Murnaghan equation of state. The crystal structure information for all the relevant phases found in this work are listed in the Supplemental Material.

[30] A. Jain, S. P. Ong, G. Hautier, W. Chen, W. D. Richards, S. Dacek, S. Cholia, D. Gunter, D. Skinner, G. Ceder, and K. A. Persson, Commentary: The materials project: A materials genome approach to accelerating materials innovation, APL Mater. **1**, 011002 (2013).

[31] J. Sun, M. Martinez-Canales, D. D. Klug, C. J. Pickard, and R. J. Needs, Persistence and Eventual Demise of Oxygen Molecules at Terapascal Pressures, Phys. Rev. Lett. **108**, 045503 (2012).

[32] H. Niu, A. R. Oganov, X.-Q. Chen, and D. Li, Prediction of novel stable compounds in the Mg-Si-O system under exoplanet pressures, Sci. Rep. **5**, 1 (2015).

[33] M. Millot, N. Dubrovinskaia, A. Černok, S. Blaha, L. Dubrovinsky, D. G. Braun, P. M. Celliers, G. W. Collins, J. H. Eggert, and R. Jeanloz, Shock compression of stishovite and melting of silica at planetary interior conditions, Science **347**, 418 (2015).

[34] C. Sotin, O. Grasset, and A. Mocquet, Mass–radius curve for extrasolar Earth-like planets and ocean planets, Icarus **191**, 337 (2007).

[35] K. Hakim, A. Rivoldini, T. Van Hoolst, S. Cottenier, J. Jaeken, T. Chust, and G. Steinle-Neumann, A new ab initio equation of state of Hcp-Fe and its implication on the interior structure and mass-radius relations of rocky super-Earths, Icarus **313**, 61 (2018).

[36] A. P. van den Berg, D. A. Yuen, K. Umemoto, M. H. G. Jacobs, and R. M. Wentzcovitch, Mass-dependent dynamics of terrestrial exoplanets using ab initio mineral properties, Icarus **317**, 412 (2019).

[37] T. Guillot, Special issue: Probing the giant planets, Phys. Today **57**, No. 4, 63 (2004).

[38] N. Nettelmann, R. Helled, J. J. Fortney, and R. Redmer, New indication for a dichotomy in the interior structure of Uranus and Neptune from the application of modified shape and rotation data, Planet. Space Sci. **77**, 143 (2013).

[39] K. Umemoto, R. M. Wentzcovitch, S. Wu, M. Ji, C.-Z. Wang, and K.-M. Ho, Phase transitions in $MgSiO_3$ post-perovskite in super-Earth mantles, Earth Planet. Sci. Lett. **478**, 40 (2017).